

# Low-Valent Nickel Thiaporphyrins. Nuclear Magnetic Resonance and Electron Paramagnetic Resonance Studies†

Piotr J. Chmielewski, Lechosław Latos-Grażyński,\* and Ewa Pacholska

Institute of Chemistry, University of Wrocław, 14 F. Joliot-Curie Street, Wrocław 50 383, Poland

Received July 23, 1993\*

The  $^2\text{H}$  NMR spectra of one-electron reduction product of nickel(II) tetraphenyl-21-thiaporphyrin have been recorded. The following selectively deuterated thiaporphyrins have been used: 5,20-diphenyl-10,15-bis(phenyl- $d_5$ )-21-thiaporphyrin (STPPH- $d_{10}$ ), 5,10,15,20-tetraphenyl-21-thiaporphyrin (STPPH- $d_6$ ) deuterated at pyrrole  $\beta$ -positions, 5,20-diphenyl-10,15-bis(*p*-tolyl)-21-thiaporphyrin (SDPDTPH- $d_2$ ) deuterated at the thiophene  $\beta$ -position. Two characteristic patterns of chemical shifts for one-electron-reduced species have been established as exemplified by Ni(STPP- $d_6$ ) (pyrrole,  $-52.3$ ,  $25.6$ ,  $21.0$  ppm; 363 K), Ni(SDPDTP- $d_2$ ) (thiophene;  $-41$  ppm; 293 K) and Ni(STPP- $d_6$ )(1-Melm) (pyrrole,  $61.3$ ,  $42.3$ ,  $20.8$  ppm; 298 K). The coordination of pyridine, methyldiphenylphosphine, and 1-methylimidazole resulted in similar spectral patterns. The  $^2\text{H}$  NMR spectra of  $\text{Cu}^{\text{II}}$ (STPP- $d_6$ ) established a standard pattern for the well-defined  $d^9$  electronic structure (pyrrole,  $49.9$ ,  $38.5$ ,  $29.6$  ppm; thiophene,  $-9.0$  ppm). The isotropic shift of nickel thiaporphyrins have been discussed in terms of the contribution of two canonical forms: nickel(I) thiaporphyrin–Ni(II) and thiaporphyrin anion radical. The  $\sigma$ - and  $\pi$ -delocalization mechanisms of the spin density have been considered to account for the isotropic shift pattern.  $^{61}\text{Ni}$  hyperfine coupling constants have been measured by means of EPR spectroscopy for the series of nickel thiaporphyrins enriched in the  $^{61}\text{Ni}$  isotope. The typical hyperfine coupling constants ( $A/10^{-4} \text{ cm}^{-1}$ ) are as follows:  $^{61}\text{Ni}$ (STPP),  $A_1 = 6.5$ ,  $A_2 = 32.2$ ,  $A_3 = 3.2$ ;  $^{61}\text{Ni}$ (STPP)( $\text{SO}_2$ ),  $A_1 = 49.3$ ,  $A_2 = 15.0$ ,  $A_3 = 18.5$ ; Ni(STPP)(1-Melm),  $A_1 = 6.9$ ,  $A_2 = 4.6$ ,  $A_3 = 16$ ;  $^{61}\text{Ni}$ (STPP)(py) $_2$ ,  $A_1 = 18.3$ ,  $A_2 = 11.1$ ,  $A_3 = 15.5$ . The coordination of  $\text{P}(\text{OEt})_3$  by Ni(STPP) has been confirmed by the characteristic superhyperfine splitting ( $A_1^{\text{P}} = 124$ ,  $A_2^{\text{P}} = 133$ ,  $A_3^{\text{P}} = 127$ ). A parallel analysis of  $^{61}\text{Ni}$  hyperfine coupling constants and  $^2\text{H}$  NMR isotropic shifts provided direct insight into the electron and spin density distribution in one-electron-reduced nickel tetraphenylthiaporphyrin complexes.

## Introduction

Mononuclear nickel(II) macrocyclic complexes undergo one-electron reductions to give nickel(I) macrocycles or nickel(II) macrocycle  $\pi$ -anion radicals. Examples of the intermediate electronic structure should be expected as well. In order to specify parameters which determine the electronic structure of these reduction products, a large variety of macrocycles including tetraaza macrocycles,<sup>1–5</sup> porphyrin,<sup>6–9</sup> isobacteriochlorin,<sup>9</sup> porphycene,<sup>10</sup> thiaporphyrins,<sup>11,12</sup> hexahydro- and octahydro-

phyrins,<sup>13</sup> and hydrocorphin in Factor F430<sup>14,15</sup> have been tested. Factor 430 (F430) was recently identified as a nickel tetrapyrrole (hydrocorphin) that comprises the prosthetic group of methyl coenzyme M reductase.<sup>16,17</sup> Detection of an EPR signal attributable to Ni(I) in the enzymatic cycles of methanogenic bacteria<sup>18</sup> has encouraged intensive investigations of the reductive chemistry of F430 and nickel(II) macrocycles.

The electronic structure assignment of reduced nickel macrocycles is usually based on EPR and UV–visible spectra.<sup>1–14</sup> Recently Ni(I) has been characterized unambiguously by EXAFS.<sup>5</sup> It is generally accepted that larger values of the  $g$  tensor unambiguously reflect the dominating contribution of a reduced nickel structure. On the other hand the  $g$  values are expected to approach 2 as the extent of delocalization of the unpaired electron

† Abbreviations: STPP, 5,10,15,20-tetraphenyl-21-thiaporphyrin anion; STTP, 5,10,15,20-tetrakis(*p*-tolyl)-21-thiaporphyrin anion; STPP- $d_{10}$ , 5,20-diphenyl-10,15-bis(phenyl- $d_5$ )-21-thiaporphyrin anion; STPP- $d_6$ , 5,10,15,20-tetraphenyl-21-thiaporphyrin anion deuterated at pyrrole  $\beta$ -positions; SDPDTP, 5,20-diphenyl-10,15-bis(*p*-tolyl)-21-thiaporphyrin anion; SDPDTP- $d_2$ , 5,20-diphenyl-10,15-bis(*p*-tolyl)-21-thiaporphyrin anion deuterated at the thiophene  $\beta$ -position;  $\text{NCH}_3\text{TTP}$ , *N*-methyltetraphenylporphyrin anion.

\* Abstract published in *Advance ACS Abstracts*, March 15, 1994.

- (1) Busch, D. H. *Acc. Chem. Res.* **1978**, *11*, 392.
- (2) Lovecchio, F. V.; Gore, E. S.; Busch, D. H. *J. Am. Chem. Soc.* **1974**, *96*, 3109.
- (3) Millar, M.; Holm, R. H. *J. Am. Chem. Soc.* **1975**, *97*, 6052.
- (4) Gagné, R. R.; Ingle, D. M. *J. Am. Chem. Soc.* **1980**, *102*, 1944. (b) Gagné, R. R.; Ingle, D. M. *Inorg. Chem.* **1981**, *20*, 420.
- (5) (a) Furenlid, L. R.; Renner, M. W.; Szalda, D. J.; Fujita, E. *J. Am. Chem. Soc.* **1991**, *113*, 883. (b) Suh, M. P.; Kim, H. K.; Kim, M. J.; Oh, K. *J. Inorg. Chem.* **1992**, *31*, 3620.
- (6) (a) Kadish, K. M.; Morrison, M. M. *Inorg. Chem.* **1976**, *16*, 980. (b) Chang, D.; Malinski, T.; Ulman, A.; Kadish, K. M. *Inorg. Chem.* **1984**, *23*, 817. (c) Kadish, K. M.; Sazou, D.; Liu, Y. M.; Saoiabi, A.; Ferhat, M.; Guillard, R. *Inorg. Chem.* **1988**, *27*, 1198. (d) Kadish, K. M.; Sazou, D.; Maiya, G. B.; Han, B. C.; Liu, Y. M.; Saoiabi, A.; Ferhat, M.; Guillard, R. *Inorg. Chem.* **1989**, *28*, 2542. (e) Kadish, K. M.; Franzen, M. M.; Han, B. C.; Araullo-McAdams, C.; Sazou, D. *J. Am. Chem. Soc.* **1991**, *113*, 512. (f) Kadish, K. M.; Franzen, M. M.; Han, B. C.; Araullo-McAdams, C.; Sazou, D. *Inorg. Chem.* **1992**, *31*, 4399.
- (7) Renner, M. W.; Forman, A.; Fajer, J.; Simpson, D.; Smith, K. M.; Barkigia, K. M. *Biophys. J.* **1988**, *53*, 277.
- (8) Lexa, D.; Mometeau, M.; Mispelter, J.; Savéant, J.-M. *Inorg. Chem.* **1989**, *28*, 30.
- (9) (a) Stolzenberg, A. M.; Stershic, M. T. *Inorg. Chem.* **1987**, *26*, 3082. (b) Stolzenberg, A. M.; Stershic, M. T. *J. Am. Chem. Soc.* **1988**, *110*, 5397. (c) Stolzenberg, A. M.; Stershic, M. T. *J. Am. Chem. Soc.* **1988**, *110*, 6391.

- (10) Furenlid, L. R.; Renner, M. W.; Smith, K. M.; Fajer, J. *J. Am. Chem. Soc.* **1990**, *112*, 1634.
- (11) (a) Chmielewski, P.; Grzeszczuk, M.; Latos-Grażyński, L.; Lisowski, J. *Inorg. Chem.* **1989**, *28*, 3546. (b) Latos-Grażyński, L.; Olmstead, M. M.; Balch, A. L. *Inorg. Chem.* **1989**, *28*, 4065.
- (12) Pandian, R. P.; Chandrashekar, T. K. *J. Chem. Soc., Dalton Trans.* **1993**, 119.
- (13) Renner, M. W.; Furenlid, L. R.; Barkigia, K. M.; Forman, A.; Shim, H.-K.; Simpson, D. J.; Smith, K. M.; Fajer, J. *J. Am. Chem. Soc.* **1991**, *113*, 6891.
- (14) Jaun, B.; Pfaltz, A. *J. Chem. Soc., Chem. Commun.* **1986**, 1327.
- (15) Hamilton, C. L.; Ma, L.; Renner, M. W.; Scott, R. A. *Biochim. Biophys. Acta* **1991**, *1074*, 312.
- (16) Ellefson, W. L.; Whitman, W. B.; Wolfe, R. S. *Proc. Natl. Acad. Sci. U.S.A.* **1982**, *79*, 3707.
- (17) (a) Pfalz, A.; Jaun, B.; Fassler, A.; Eschenmoser, A.; Jaenchen, R.; Gilles, H. H.; Diekert, G.; Thauer, R. R. *Helv. Chim. Acta* **1982**, *65*, 828. (b) Livingston, D. A.; Pfaltz, A.; Schreiber, J.; Eschenmoser, A.; Ankel-Fusch, D.; Moll, J.; Jaenchen, R.; Thauer, R. K. *Helv. Chim. Acta* **1984**, *67*, 334. (c) Pfaltz, A.; Livingston, D. A.; Jaun, B.; Diekert, G.; Thauer, R.; Eschenmoser, A. *Helv. Chim. Acta* **1985**, *65*, 1338. (d) Pfaltz, A. In *The Bioinorganic Chemistry of Nickel*; Lancaster, J. R., Jr., Ed.; VCH Publishers Inc.: New York, 1988; p 275.
- (18) (a) Albracht, S. P. J.; Ankel-Fusch, D.; Van der Zwaan, J. W.; Fontijn, R. D.; Thauer, R. K. *Biochim. Biophys. Acta* **1986**, *870*, 50. (b) Albracht, S. P. J.; Ankel-Fusch, D.; Boecher, R.; Ellerman, J.; Moll, J.; Van der Zwaan, J. W.; Thauer, J. K. *Biochim. Biophys. Acta* **1988**, *955*, 86.

from the metal atom increases.<sup>19</sup> To gain better insight into a description of the electronic ground state and the related electron/spin density distribution in nickel macrocycles, we have decided to use EPR and extend the set of measurable parameters to include hyperfine coupling constants of the <sup>61</sup>Ni isotope ( $I = 3/2$ ). Since the <sup>61</sup>Ni isotope has a natural abundance of 1%, selected experiments in this paper have been carried out with <sup>61</sup>Ni(STPP) isotope enriched samples (90% <sup>61</sup>Ni). One can treat <sup>61</sup>Ni hyperfine coupling constants as a sensitive probe of the electronic and ligation states of nickel in reducing conditions. In principle, a set of hyperfine coupling constants should allow the estimation of the distribution of the unpaired electron between the ligand and nickel d orbitals.<sup>19-21</sup> Previously we have investigated one-electron reduction of nickel(II) thiaporphyrins by means of EPR spectroscopy. We have established a profound impact of axial ligation on the principal values of the **g** tensor.<sup>11</sup> Well-resolved EPR spectra suggest that <sup>1</sup>H NMR resonances of the studied species can be beyond detection as  $T_{1\rho}$  is relatively long.<sup>22,23</sup> Resonances of pyrrole and *meso*-phenyl protons of paramagnetic metalloporphyrins have been shown to be particularly diagnostic of changes of spin, oxidation, and ligation states in metalloporphyrins and their radicals.<sup>22</sup> We have examined <sup>2</sup>H NMR spectra to get some insight into the spin density distribution in a macrocyclic core using specifically deuterated nickel thiaporphyrins. In the limit of electron-nuclear dipolar relaxation, line widths for deuterium resonances are theoretically predicted to be 42 times smaller than the corresponding proton resonances.<sup>23</sup> The essential narrowing has been observed experimentally for many paramagnetic species and renders <sup>2</sup>H NMR spectroscopy particularly useful in detecting those paramagnetically broadened resonances that are not accessible in <sup>1</sup>H NMR.<sup>24,25</sup>

The electronic structure of other d<sup>9</sup> systems, i.e. the respective Cu(II) complexes, is definitely far better understood than their Ni(I) counterparts. For this reason the corresponding <sup>2</sup>H NMR spectra have also been analyzed. <sup>2</sup>H NMR patterns of copper(II) complexes are more likely to be associated with a well-defined electronic configuration and are expected to be suitable spectroscopic models for one-electron reduced nickel(II) macrocyclic complexes.

## Results

**NMR Studies of Nickel Complexes.** Chemical reduction of Ni<sup>II</sup>(STPP-*d*<sub>6</sub>)Cl by sodium anthracenide in THF was monitored by deuterium NMR spectroscopy. Titration of a 5 mM solution of Ni<sup>II</sup>(STPP-*d*<sub>6</sub>)Cl yield the same spectroscopically identified product as that obtained by reduction with tetrabutylammonium borohydride in toluene or by preparative reduction with zinc

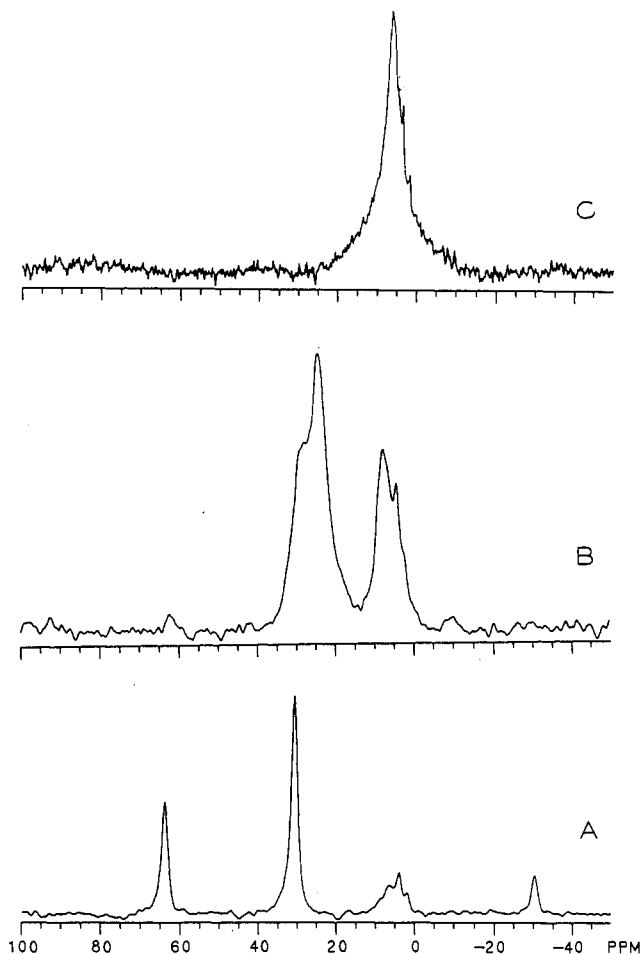
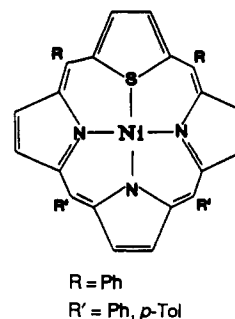


**Figure 1.** <sup>2</sup>H NMR titration of Ni<sup>II</sup>(STPP-*d*<sub>6</sub>)Cl with sodium anthracenide (THF, 298 K). Number of equivalents added: (A) 0; (B) 1; (C) 2.

amalgam.<sup>11</sup> In addition the two-electron reduced species was also observed with pyrrole resonances at 7 ppm. We have also noticed that Ni<sup>II</sup>(STPP)Cl is reduced by OH<sup>-</sup> in THF/H<sub>2</sub>O. The results of titration with sodium anthracenide are shown in Figure 1. In both cases the reduction can be reversed by treating the reduced species with I<sub>2</sub>. The axial chloride ligand is removed from the coordination sphere in the course of reduction. The <sup>2</sup>H NMR spectrum of the reoxidized product (pyrroles, 65.7, 55.22, 26.3; thiophene, -19.8 ppm; 298 K) corresponds to the six-coordinate species and likely has two THF molecules occupying the axial positions.<sup>26</sup>

The NMR data have been analyzed on the presumption that the effective C<sub>2</sub> geometry is adequate to describe reduced complexes.<sup>11b</sup>



There are three distinct pyrrole positions, one thiophene position, and two *meso* positions. With phenyl rings in both of

- (19) (a) Geiger, W. E., Jr.; Allen, C. S.; Mines, T. E. *Sentfleber, F. C. Inorg. Chem.* **1977**, *16*, 2003. (b) Bowmaker, G. A.; Boyd, P. D. W.; Campbell, G. K. *Inorg. Chem.* **1982**, *21*, 2403. (c) Bowmaker, G. A.; Boyd, P. D. W.; Campbell, G. K.; Hope, J. M.; Martin, R. L. *Inorg. Chem.* **1982**, *21*, 1152. (d) Bowmaker, G. A.; Boyd, P. D. W.; Zvagulis, M.; Cavell, K. J.; Masters, A. F. *Inorg. Chem.* **1985**, *24*, 401. (e) Bowmaker, G. A.; Boyd, P. D. W.; Campbell, G. K.; Zvagulis, M. *J. Chem. Soc., Dalton Trans.* **1986**, 1065.
- (20) (a) Saraev, V. V.; Ri, B.; Shmidt, F. K.; Larin, G. M. *Koord. Khim.* **1982**, *48*, 1485. (b) Gruznykh, V. A.; Saraev, V. V.; Shmidt, F. K.; Larin, G. M. *Koord. Khim.* **1983**, *9*, 1400. (c) Saraev, V. V.; Shmidt, F. K. *Koord. Khim.* **1986**, *12*, 347.
- (21) (a) Attanasio, D. *J. Magn. Reson.* **1977**, *26*, 81. (b) Attanasio, D.; Collamati, I.; Cervone, E. *Inorg. Chem.* **1983**, *22*, 3281. (c) Agostinelli, E.; Attanasio, D.; Collamati, I.; Fares, V. *Inorg. Chem.* **1984**, *23*, 1162.
- (22) (a) La Mar, Walker, F. A. In *Porphyrins*; Dolphin, D., Ed., Academic Press: New York, 1979; Vol. IVB, p 61. (b) Bertini, I.; Luchinat, C. *NMR of Paramagnetic Molecules in Biological Systems*; The Benjamin/Cumming Publishing Co., Inc.: Menlo Park, CA, 1986. (c) Goff, H. M. In *Iron Porphyrins, Part I*; Lever, A. B. P., Gray, H. B., Eds.; Addison-Wesley: Reading, MA, 1983; p 237.
- (23) Swift, T. J. In *NMR of Paramagnetic Molecules*; La Mar, G. N., Horrocks, W. DeW., Holm, R. H., Eds.; Academic Press: New York, 1973; p 53.
- (24) Hickaman, D. L.; Shirazi, A. Goff, H. M. *Inorg. Chem.* **1985**, *24*, 563.
- (25) Balch, A. L.; La Mar, G. N.; Latos-Grażyński, L.; Renner, M. W. *Inorg. Chem.* **1985**, *24*, 2432.

- (26) Lisowski, J.; Latos-Grażyński, L.; Sztterenber, L. *Inorg. Chem.* **1992**, *31*, 1933.

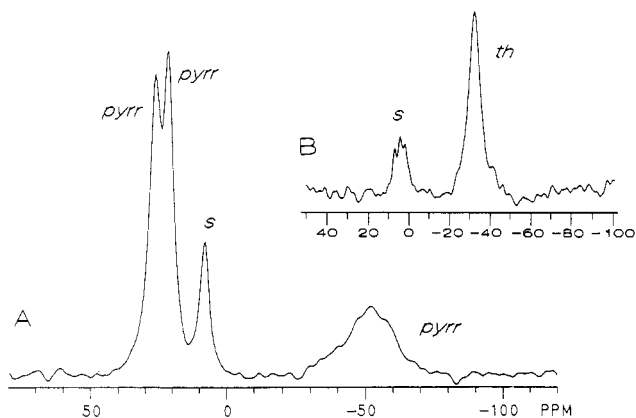


**Figure 2.**  $^2\text{H}$  NMR spectra of Ni(STPP- $d_6$ ) (A) and Ni(SDPDTP- $d_2$ ) (B). Both spectra were measured in toluene solutions at 363 K. Labeling: pyrr, pyrrole; th, thiophene, s, solvent.

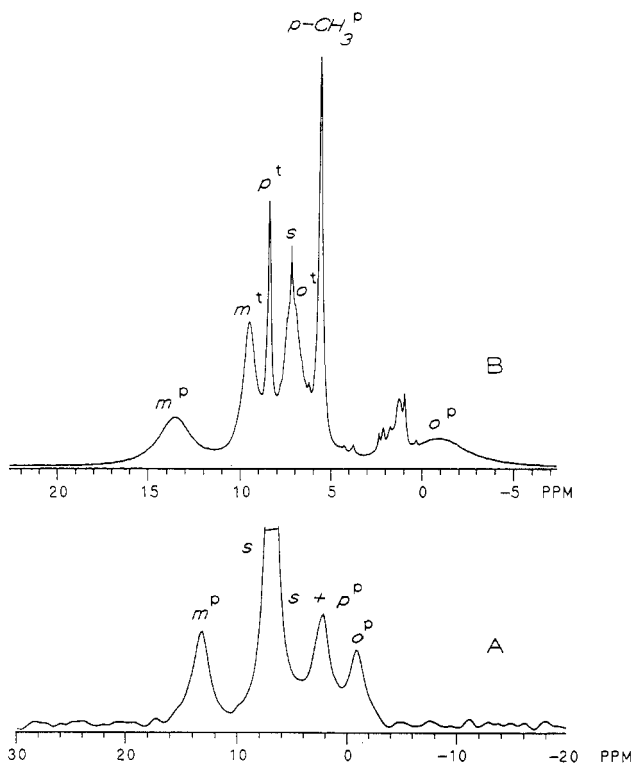


**Figure 3.** NMR spectra at 298 K: (A) Ni(STPP- $d_{10}$ ) in toluene,  $^2\text{H}$  NMR; (B) Ni(SDPDTP) in toluene- $d_8$ ,  $^1\text{H}$  NMR. Resonance assignments: o, ortho; m, meta; p, para; s, solvent. Superscripts t and p identify 5,20- and 10,15-phenyl rings respectively.

the two *meso* positions, it may be anticipated that *ortho* and *meta* positions on each ring will be distinguishable due to the nearly perpendicular relationship between the phenyl plane and the nearest pyrrole plane if the rotation about the *meso* carbon-phenyl bond is restricted.

Representative NMR data are presented in Figures 2–5 and in Tables 1 and 2. Resonance assignments are straightforward as samples for  $^2\text{H}$  NMR have to be selectively deuterated. Trace A of Figure 2 shows a sample of the material with specific deuteration of the pyrrole positions and accidental deuteration (10%) of the thiophene one. Only two downfield pyrrole resonances have been identified at 298 K. The third one is upfield shifted and this feature can be observed only at elevated temperatures due to its enormously large line width (780 Hz at 363 K) (Figure 2, Trace A). The broad thiophene resonance has been readily identified in the  $^2\text{H}$  NMR spectrum of the species selectively deuterated at the thiophene moiety Ni(SDPDTP- $d_2$ ) (Figure 2, Trace B).

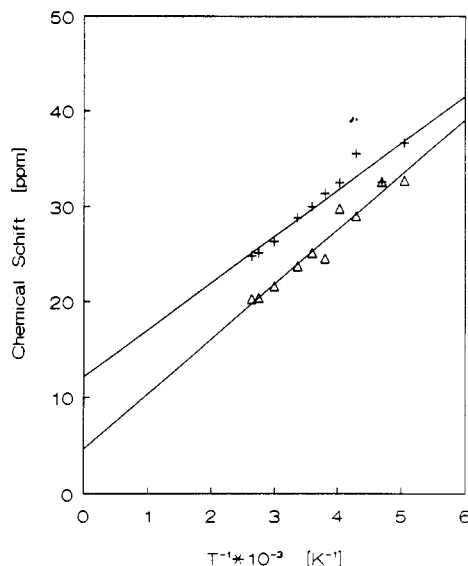


**Figure 4.** Curie plots of pyrrole protons of Ni(STPP- $d_6$ ) in toluene.

Figure 3 shows the  $^2\text{H}$  NMR spectrum of Ni(STPP- $d_{10}$ ) and the  $^1\text{H}$  NMR spectrum of Ni(SDPDTP). A downfield resonance in trace A has been assigned to the *meta* 10,15-phenyl protons. The respective *ortho* and *para* resonances (as distinguished by their intensities) are shifted upfield.  $^1\text{H}$  NMR resonances of phenyl protons are relatively narrow and could be directly analyzed and assigned to 5,20-phenyls. The same pattern, i.e. downfield *meta* and upfield *ortho*, has also been determined, but their shift values are smaller. The *para* methyl resonance (10,15-phenyl of Ni(SDPDTP)), could be easily identified, and its isotropic shift has the opposite sign as the *para* proton in the same position. The rotation of the phenyl ring with respect to the *meso* carbon-phenyl bond is fast even at 298 K as single *ortho* and *meta* resonances are observed similar to the case of Ni<sup>II</sup>(STPP)-Cl.<sup>26</sup>

A Curie plot for the pyrrole resonances is shown in Figure 4. Each resonance displays linear behavior with the extrapolated shifts at infinite temperature near the anticipated diamagnetic reference positions (Table 1).

As we have previously determined by means of EPR, Ni(STPP) has an extremely low affinity for coordination of axial ligands at 298 K.<sup>11a</sup> Addition of equimolar amounts of pyridine or 1-methylimidazole to a THF solution of Ni(STPP) at 298 K does not produce noticeable changes in the spectrum unless the compound is dissolved in pyridine itself or in a 50/50 v/v mixture of pyridine/THF (Table 1). We ascribe this remarkable shift of the upfield pyrrole resonance in the downfield direction to the formation of the adducts Ni(STPP- $d_6$ )(py)<sub>*n*</sub> (*n* = 1,2). The adducts remain in fast exchange with four-coordinate species. The temperature dependence of the pyrrole chemical shifts shows a sigmoidal type relationship (inset in Figure 5). The unusual sign change for one (formerly upfield) pyrrole resonance allows the determination of a limiting value for the pyrrole shifts of the pyridine coordinated species at 233 K (Figure 5, Table 1). This can be extrapolated at 298 K, based on the Curie law, to give chemical shifts of 75.7, 42.3, and 23.3 ppm respectively. As the smooth change of the shifts has been observed, the direct correspondence between pyrrole resonances could be established. These observations suggest that axial coordination results in a sign flip of the unique pyrrole resonance. The sign of the thiophene paramagnetic shift is preserved after axial coordination, but its value is smaller compared to the four-coordinate species (Table 1).

The  $^2\text{H}$  NMR spectra of Ni(STPP- $d_6$ ) in neat 1-MeIm or in toluene with an excess of SO<sub>2</sub> exhibit patterns similar to those

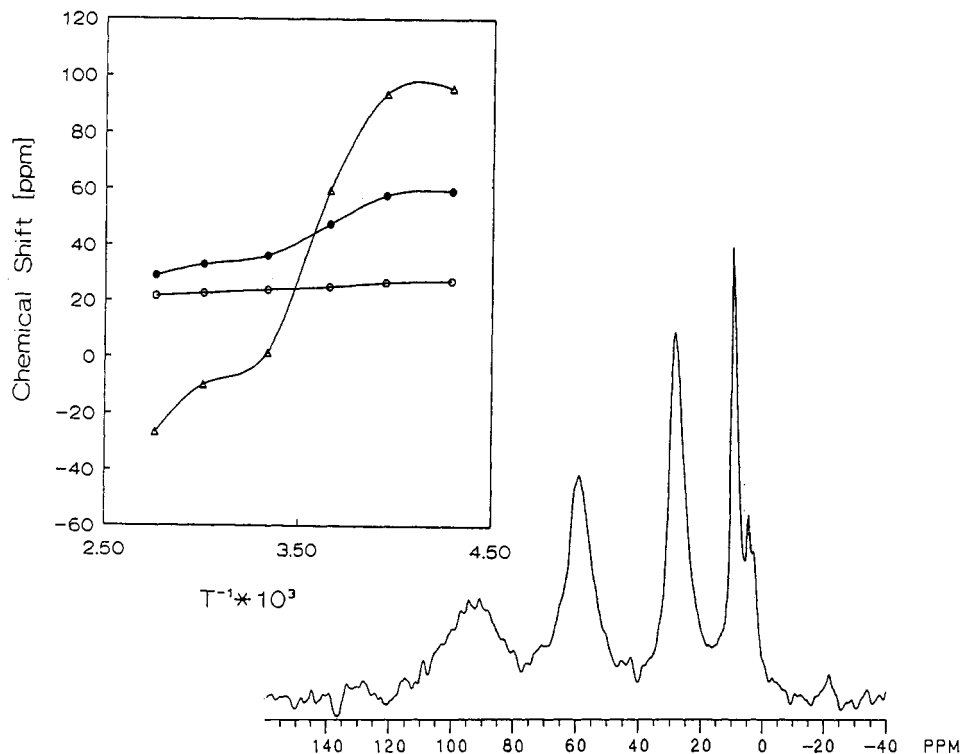


Figure 5.  $^2\text{H}$  NMR spectrum of  $\text{Ni}(\text{STPP-}d_6)$  dissolved in a pyridine/THF mixture (50/50 v/v). The corresponding temperature dependences of the chemical shifts are presented in the inset.

Table 1.  $^1\text{H}$  NMR and  $^2\text{H}$  NMR Chemical Shifts of Pyrrole and Thiophene Resonances for Nickel and Copper Thiaporphyrins

compound	T (K)	resonances		
		pyrrole		thiophene
$\text{Ni}(\text{STPP-}d_6)^a$	298	-66.5 <sup>b</sup>	28.8 (230)	23.7 (150)
	363	-52.3 (780)	25.6 (160)	21.0 (130)
$\text{Ni}(\text{SDPDTP-}d_2)$	293			-41 (800)
$\text{Ni}(\text{STPP-}d_6)(1\text{-MeIm})^c$	298	61.3	42.3	20.8
$\text{Ni}(\text{STPP-}d_6)\text{py}^d$	298	1.4	36.2	23.9
	298 <sup>e</sup>	75.7 <sup>e</sup>	42.3 <sup>e</sup>	23.3 <sup>e</sup>
	233	94.4 (840)	59.4 (395)	27.3 (200)
$\text{Ni}(\text{SDPDTP-}d_2)^d$	293			-21
$\text{Ni}(\text{STPP-}d_6)(\text{SO}_2)^{e,f}$	298	-8.3	40	30.8
$\text{Ni}(\text{STPP-}d_6)(\text{SO}_2)^{e,g}$	298	67.8	50	35.7
$\text{Ni}(\text{STPP})(\text{PMePh}_2)^h$	298	-43.3	30.0	24.5
$\text{Cu}^{\text{II}}(\text{STPP})\text{Cl}^a$	298	49.9	38.5	29.6
$\text{Cu}^{\text{II}}(\text{STPP})\text{ClO}_4$	333		33	-4.2
$\text{Ni}^{\text{II}}(\text{STPP-}d_6)\text{Cl}^i$	298	62.8	30.1	30.1
$\text{Ni}^{\text{II}}(\text{STPP})\text{Cl}^j$	298	65.5	32.5	35.8
$[\text{Ni}^{\text{II}}(\text{STPP})(1\text{-MeIm})]\text{Cl}^j$	298	65.2	32.8	35.5
$[\text{Ni}^{\text{II}}(\text{STPP})(1\text{-MeIm})_2]\text{Cl}^j$	298	70.5	35.5	54.0
$\text{Ni}^{\text{II}}(\text{STPP})(p\text{-tolyl})^k$	203	87.0	33.9	-1.4
$[\text{Zn}(\text{TPP}^*)]^{-l}$		-18		
$\text{Pd}^{\text{II}}(\text{STPP})\text{Cl}^m$		9.994	8.970	8.804
				9.783

<sup>a</sup> In toluene. <sup>b</sup> Evaluated, assuming Curie dependence, based on the shift at 363 K. <sup>c</sup> In net 1-MeIm. <sup>d</sup> In THF/pyridine 50/50 v/v. <sup>e</sup> Evaluated, assuming Curie dependence, based on the shift at 243 K. <sup>f</sup> Small amount of  $\text{SO}_2$  added. <sup>g</sup> An excess of  $\text{SO}_2$  added. <sup>h</sup> In the toluene/ $\text{PMePh}_2$  50/50 v/v mixture. <sup>i</sup> THF. <sup>j</sup> From ref 26. <sup>k</sup> From ref 32. <sup>l</sup> From ref 24. <sup>m</sup> The shifts of  $\text{Pd}^{\text{II}}(\text{STPP})\text{Cl}$  have been used as diamagnetic reference: Lisowski, J. Ph.D. Thesis University of Wrocław, 1991. <sup>n</sup> Line widths in Hz are given in parentheses.

for the low-temperature pyridine species and resemble those of high-spin nickel(II) thiaporphyrins (Table 1). Generally, the coordination of axial ligands decreased the magnitude of the chemical shifts of the phenyl resonances while preserving the sign.

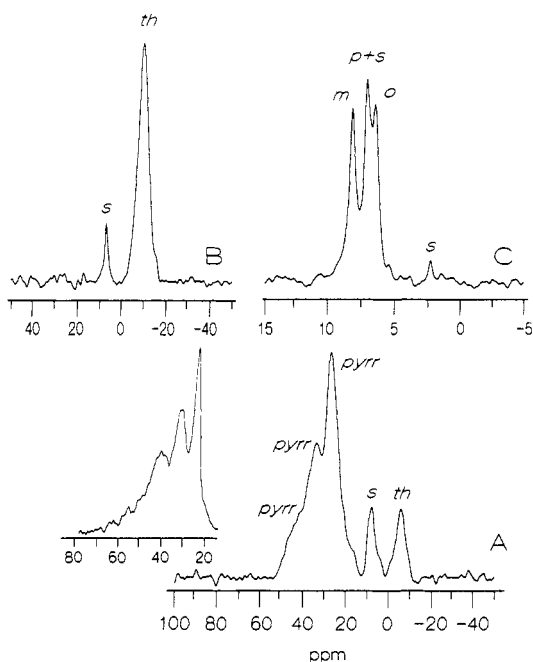
The addition of methyldiphenylphosphine has also been followed at 298 K. A similar behavior of the upfield pyrrole to that seen in the pyridine case has been established. The upfield resonance moved downfield (20 ppm). Under these experimental conditions, we could not reach the limiting values of the shifts. The downfield pyrrole resonances demonstrated rather minor changes.

**NMR Studies of Copper(II) Complexes.** The  $^2\text{H}$  NMR spectra of  $\text{Cu}^{\text{II}}(\text{STPP-}d_6)\text{Cl}$ ,  $\text{Cu}^{\text{II}}(\text{STPP-}d_{10})$ , and  $\text{Cu}^{\text{II}}(\text{STPP-}d_2)\text{Cl}$  are shown in Figure 6.  $\text{Cu}^{\text{II}}(\text{STPP-}d_6)\text{Cl}$  in toluene exhibit three pyrrole resonances at 50.0, 38.5, and 29.6 ppm at 298 K. In addition, the upfield resonance of thiophene at -9.0 ppm has been identified which results from the partial deuteration at this position during the synthesis of  $\text{STPPH-}d_6$ . This assignment has been unambiguously confirmed by the  $^2\text{H}$  NMR spectrum of  $\text{Cu}^{\text{II}}(\text{SDPDTP-}d_2)\text{Cl}$ . The phenyl resonances are clustered around 7.5 ppm showing the shift pattern typical of  $\pi$ -delocalization, i.e. *meta*, downfield; *ortho* and *para* resonances upfield with respect to their diamagnetic references.

**Table 2.**  $^1\text{H}$  NMR and  $^2\text{H}$  NMR Chemical Shifts of Phenyl Resonances for Nickel and Copper Thiaporphyrins<sup>a</sup>

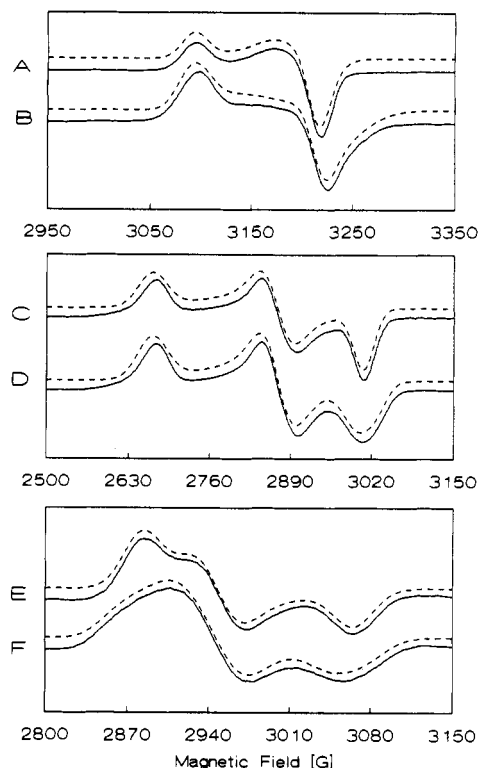
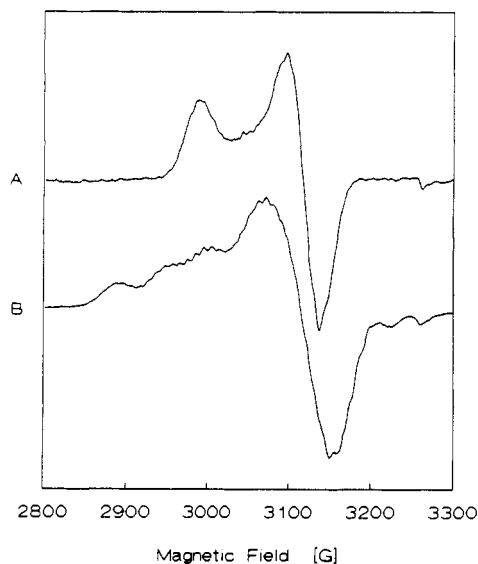
compound	T (K)	phenyl resonances		
		meta	ortho	para
Ni(STPP- <i>d</i> <sub>10</sub> )	293	13.1	-0.9	2.2
Ni(SDPDTP)	293			
10,15-phenyl		13.6	-1.0	(5.5) <sup>b</sup>
5,20-phenyl		9.5	7.1	8.3
Ni(STPP- <i>d</i> <sub>10</sub> )py <sup>d</sup>	293	9.4	6.1	5.0
Ni(STPP- <i>d</i> <sub>10</sub> )(SO <sub>2</sub> ) <sup>d</sup>	293	10.9	2.3	4.6
Cu <sup>II</sup> (STPP- <i>d</i> <sub>10</sub> )Cl	293	8.3	5.9	6.6
Cu <sup>II</sup> (STPP- <i>d</i> <sub>10</sub> )Cl	333	8.2	6.6	7.0
Cu <sup>II</sup> (STPP- <i>d</i> <sub>10</sub> )(ClO <sub>4</sub> ) <sup>d</sup>	333	8.7	6.2	6.8
Ni <sup>II</sup> (STPP- <i>d</i> <sub>10</sub> )Cl	293			
5,20-phenyl		9.9	7.3	6.2
10,15-phenyl		9.7	8.1	7.5
[ZnTPP] <sup>-c,d</sup>	298	10.0	1.0	6.5
Pd <sup>II</sup> (STPP)Cl <sup>e</sup>				
5,20-phenyl		7.93	8.37	7.91
10,15-phenyl		7.63	8.058	(2.71)

<sup>a</sup> In toluene, 298 K. <sup>b</sup> *p*-CH<sub>3</sub>. <sup>c</sup> From ref 24. <sup>d</sup> The positions do not represent limiting values for a pure form. The spectrum was taken in a pyridine/toluene mixture (50/50 v/v). <sup>e</sup> The shifts of Pd<sup>II</sup>(STPP)Cl have been used as a diamagnetic reference.

**Figure 6.**  $^2\text{H}$  NMR spectra: (A) Cu<sup>II</sup>(STPP-*d*<sub>6</sub>)Cl (333 K (inset 363 K, C<sub>7</sub>H<sub>8</sub>)); (B) Cu<sup>II</sup>(SDPDTP-*d*<sub>2</sub>) (298 K, CHCl<sub>3</sub>); (C) Cu<sup>II</sup>(STPP-*d*<sub>10</sub>)Cl (333 K C<sub>7</sub>H<sub>8</sub>). Peak assignments follow those from the previous figures.

**EPR Spectra.** Previously we have demonstrated the characteristic EPR spectra of Ni(STPP)L<sub>*n*</sub> ( $^{58}\text{Ni}$ ).<sup>11a</sup> For the sake of consideration in this paper, we present the most relevant examples of EPR spectra measured under identical conditions for  $^{58}\text{Ni}$ (STPP) and  $^{61}\text{Ni}$ (STPP). Such direct comparison allows the elucidation of the impact of the isotope substitution on the EPR spectral pattern. The simulated features are shown in selected examples (Figures 7–9). The characteristic values which include hyperfine coupling constants are gathered in Table 3.

The spectra of  $^{61}\text{Ni}$ (STPP)(P(OEt)<sub>3</sub>);  $^{61}\text{Ni}$ (STPP)(1,2-diMeIm);  $^{61}\text{Ni}$ (STPP)(py)<sub>2</sub> definitely exhibit rhombic *g* tensors ( $g_1 - g_2 \cong g_2 - g_3$ ) and a strongly reduced anisotropy of the  $^{61}\text{Ni}$  hyperfine tensor. These features are typical for a very low symmetry environment with extensive mixing of d orbitals in the ground state.<sup>21</sup> The measured hyperfine coupling constants are rather small but comparable with other  $^{61}\text{Ni}$ (I) compounds (Table 3). The best resolved hyperfine pattern has been observed for the SO<sub>2</sub> adduct (Figure 8).

**Figure 7.** EPR spectra (X-band, 77 K, toluene): (A)  $^{58}\text{Ni}$ (STPP); (B)  $^{61}\text{Ni}$ (STPP); (C)  $^{58}\text{Ni}$ (STPP)(1,2-diMeIm); (D)  $^{61}\text{Ni}$ (STPP)(1,2-diMeIm); (E)  $^{58}\text{Ni}$ (STPP)(py)<sub>2</sub>; (F)  $^{61}\text{Ni}$ (STPP)(py)<sub>2</sub>. The solid lines correspond to the experimental spectra. The simulated spectra are shown as dashed lines.**Figure 8.** EPR spectra (77 K, toluene): (A)  $^{58}\text{Ni}$ (STPP)(SO<sub>2</sub>); (B)  $^{61}\text{Ni}$ (STPP)(SO<sub>2</sub>). The superhyperfine coupling to the pyrrole nitrogens is also observed in trace B.

In a search for other spectroscopic probes of the nickel ion electronic state, the superhyperfine coupling constants to  $^{31}\text{P}$  of the phosphines (PMePh<sub>2</sub>, PEtPh<sub>2</sub>) and phosphite (P(OEt)<sub>3</sub>) ligands have been investigated (Figure 9, Table 3). The spectra clearly correspond to five-coordinate species as a coupling to only one phosphorus atom has been established. However, the *g* tensor values are different from those established for five-coordinate species with a nitrogen base located in the axial position.

## Discussion

**Analysis of EPR Parameters.** MO theoretical considerations suggest that for *d*<sup>9</sup> configurations the singly-occupied molecular

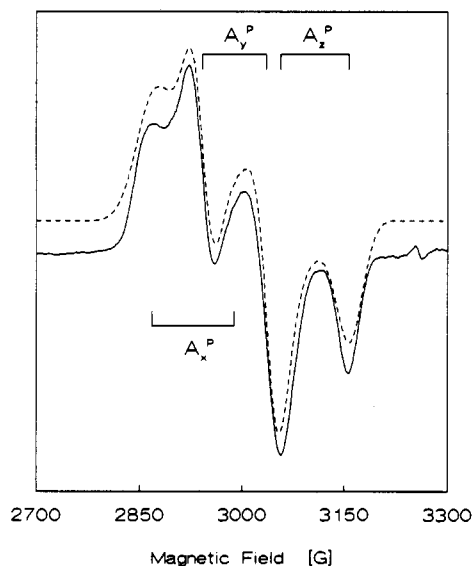


**Figure 9.** EPR spectrum (77 K, toluene) of  $^{58}\text{Ni}(\text{STPP})(\text{PEtPh}_2)$ . The  $^{31}\text{P}$  superhyperfine coupling scheme is shown. The solid lines correspond to the experimental spectrum. The simulated spectrum is shown as a dashed line.

orbital can be expressed as<sup>20</sup>

$$\psi_{\text{SOMO}} = \alpha\psi_{x^2-y^2} + (1 - \alpha^2)^{1/2}\psi_L \quad (1)$$

where

$$\psi_{x^2-y^2} = a d_{x^2-y^2} + b d_{z^2} \quad (2)$$

and  $\psi_L$  is the molecular orbital of the ligand. The covalency parameter  $\alpha^2$  is related to the EPR spectral parameters. We have made an attempt to estimate  $\alpha^2$  using previously described procedures.<sup>20</sup> However we have encountered several limitations imposed by the investigated systems and the respective calculation should be treated only qualitatively.

In two cases the  $A_{\text{iso}}$  values were available ( $^{61}\text{Ni}(\text{STPP})$ ,  $^{61}\text{Ni}(\text{STPP})(\text{SO}_2)$ ) while the other five- and six-coordinate forms gave EPR spectra only in frozen solutions. For this reason the relative signs of  $A_i$  components could be established only for  $^{61}\text{Ni}(\text{STPP})$  and  $^{61}\text{Ni}(\text{STPP})\text{SO}_2$ .

The orientations of out-of-plane  $g$  tensor components for selected nickel(I) thiaporphyryns with respect to the molecular coordinate system have been previously analyzed by means of measurements in the frozen nematic, oriented phases of the liquid crystals.<sup>11</sup> These data have been used as a starting point for our analysis, but we have examined all possible combinations of the orientation  $g$  and  $A$  tensors with respect to the molecular frame. The relative signs of  $A_i$  were varied as well. Only the sets of parameters which produced negative  $P$  values ( $P_0(^{61}\text{Ni}) = -102 \times 10^{-4} \text{ cm}^{-1}$ <sup>27</sup>) have been considered. The estimated covalency factor varies in the range 0.3–0.5 for all investigated species. The method of Swallen and co-workers for calculating bonding parameters from the EPR data gave similar results.<sup>28</sup>

The EPR spectra of Ni(I) species have been investigated far less than those of the isoelectronic  $d^9$  copper(II) since Ni(I) species are much less common. The available data which include  $^{61}\text{Ni}$  hyperfine coupling constants are very limited.<sup>8,18,19a,b</sup> Only two cases of a  $^{61}\text{Ni}(\text{I})$  ion in a macrocyclic environment have been reported.<sup>8,18</sup> In both the hyperfine coupling is relatively small and is reported only as some broadening of the  $^{61}\text{Ni}$  spectrum as compared to the  $^{58}\text{Ni}$  one. We would like to point out that we tested this procedure for the parameters ( $g_i, A(^{61}\text{Ni})$ ) reported

in the literature, receiving an essentially identical estimation of the covalency factor  $\alpha^2$ .<sup>19a,b</sup> An identical approach to the  $\text{Cu}^{\text{II}}(\text{STPP})\text{Cl}$  spectrum resulted in  $\alpha^2 = 0.78$ , which is in the characteristic range for copper(II) porphyrins.<sup>29</sup>

In general the  $\alpha^2$  covalency factor decreases in the case of nickel thiaporphyryns as compared to analogous copper(II) complexes. It seems that the best description of the electron distribution in one-electron-reduced nickel thiaporphyryns requires a molecular orbital which allows for substantial spin density simultaneously on the nickel ion and thiaporphyrin. This description is consistent with the low symmetry allowing strong overlap between ( $ad_{x^2-y^2} + bd_{z^2}$ ) metal orbitals and  $\sigma$ ,  $\pi$ , and  $\pi^*$  orbitals of the thiaporphyrin. Even relatively low contribution of metal orbitals in the electronic ground-state orbital produces anisotropic EPR spectra routinely described as typical for the Ni(I)  $d^9$  electronic structure. Other criteria such as hyperfine  $^{61}\text{Ni}$  coupling constants, superhyperfine coupling constants of axial or equatorial ligands, and reactivity characteristics for the Ni(I) center should be carefully applied. In our systems the relatively large hyperfine coupling constants of  $^{31}\text{P}$  suggest considerable Ni(I) character at Ni(STPP)(P(OEt)<sub>3</sub>), Ni(STPP)(PMePh<sub>2</sub>), and Ni(STPP)(PEtPh<sub>2</sub>). Structural parameters of Ni(STPP) are also consistent with the contribution of the  $d^9$  electronic structure.<sup>11</sup>

**Analysis of NMR Spectra.** The relationship between the isotropic shift pattern and the electronic structure of paramagnetic metalloporphyrins as measured by means of NMR has been well established and used with success to discuss the electronic structure of oxidized and reduced metalloporphyrins.<sup>22</sup> Qualitative information on the nature of metal ion–porphyrin bonding is contained in the contact shift contribution to the isotropic shift. Some dipolar contribution can be expected for nickel(I) and copper(II) thiaporphyryns since the well-defined anisotropy of the  $g$  tensor has been established in each case studied. If the dipolar contribution is dominating, the relative geometric factors for the three phenyl substituents demand dipolar shifts in the same directions and relative magnitudes with  $o\text{-H} > m\text{-H} > p\text{-H}$ .<sup>22</sup> The observed patterns of the phenyl resonances in all  $d^9$  systems under investigation present the alternation of shift direction for the phenyl protons. The  $p$ -methyl group exhibits a shift of the opposite sign to that established for the *para* proton. This is characteristic for the domination of  $\pi$ -contact shift. Phenyl ring rotation allows  $\pi$ -spin density delocalization onto the rings by removing the orthogonality of the phenyl and porphyrin  $\pi$ -systems. The domination of the contact shift in the phenyl groups precludes calculation of the dipolar contribution at other, usually less insulated, positions. Consequently the dipolar contribution to the isotropic shift of pyrrole and thiophene resonances is expected to be negligible and the measured isotropic shift is a direct indication of the spin delocalization in the thiaporphyrin skeleton. Plots of  $^2\text{H}$  NMR line widths of the pyrrole resonances of (Ni(STPP- $d_6$ ), Ni(STPP- $d_6$ )(1-MeIm), Ni(STPP- $d_6$ )py, and  $\text{Cu}^{\text{II}}(\text{STPP-}d_6)\text{Cl}$ ) vs the square of the contact shifts are linear. The fact that these plots have a significant slope indicates that there is a prominent contribution of scalar relaxation to the linewidth of the pyrrole and phenyl resonances.

The downfield shift of pyrrole resonances is indicative of  $\sigma$ -delocalization of spin density and is consistent with the ground state of Ni(I) or Cu(II) which have unpaired electrons in the  $\sigma$ -symmetry orbitals ( $ad_{x^2-y^2} + bd_{z^2}$ ). Similar trends are established for  $\text{Cu}^{\text{II}}(\text{TPP})$ .<sup>30</sup> A large difference in contact shifts of pyrrole resonances is seen even for protons located on the same pyrrole ring. Three well-separated pyrrole resonances, in the limit of complete axial coordination, have been observed for  $\text{Cu}^{\text{II}}(\text{STPP-}d_6)\text{Cl}$ , Ni(STPP- $d_6$ ), Ni(STPP- $d_6$ )(1-MeIm), and Ni(STPP- $d_6$ )(SO<sub>2</sub>).

(27) Morton, J. R.; Preston, K. F. *J. Magn. Reson.* **1978**, *30*, 577.

(28) Swallen, J. D.; Johnson, B.; Gladney, H. M. *J. Chem. Phys.* **1970**, *52*, 4078.

(29) Lisowski, L.; Grzeszczuk, M.; Latos-Grażyński, L. *Inorg. Chim. Acta* **1989**, *161*, 153–63.

(30) Godziela, G. M.; Goff, H. M. *J. Am. Chem. Soc.* **1986**, *108*, 2237.

Table 3. EPR Parameters of  $^{61}\text{Ni}(\text{STPP})$  Complexes<sup>a</sup>

	Ni(STPP)	Ni(STPP)SO <sub>2</sub>	Ni(STPP)P(OEt) <sub>3</sub>	Ni(STPP)- PMePh <sub>2</sub>	Ni(STPP)- PEtPh <sub>2</sub>	Ni(STPP)- 1,2-MeIm	Ni(STPP)py	[Ni(Bu <sub>2</sub> NCS) <sub>2</sub> ] <sup>-</sup>		[Ni(mnt) <sub>2</sub> ] <sup>3-c</sup>
								I <sup>b</sup>	II <sup>b</sup>	
<i>g</i> <sub>1</sub>	2.109	2.188	2.242	2.266	2.240	2.417	2.260	2.272	2.260	2.205
<i>g</i> <sub>2</sub>	2.039	2.096	2.184	2.192	2.183	2.246	2.210	2.062	2.207	2.081
<i>g</i> <sub>3</sub>	2.031	2.071	2.097	2.100	2.107	2.142	2.127	2.062	2.025	2.061
<i>g</i> <sub>iso</sub>	2.059	2.115								
<i>g</i> <sub>av</sub>	2.060	2.118	2.174	2.189	2.177	2.268	2.199	2.132	2.164	2.116
<i>A</i> <sub>1</sub>	6.5	49.3	12.1	10.7		6.9	18.3	53	13	53
<i>A</i> <sub>2</sub>	32.2	15.0	18.9	20.9		4.6	11.1	9	13	6
<i>A</i> <sub>3</sub>	3.2	18.5	12.3	12.7		16.0	15.5	9	16.5	6
<i>A</i> <sub>iso</sub>	12.0	27.3								
<i>A</i> <sub>1</sub> <sup>P</sup>			124	76	116					
<i>A</i> <sub>2</sub> <sup>P</sup>			133	83	101					
<i>A</i> <sub>3</sub> <sup>P</sup>			127	73	101					

<sup>a</sup> Hyperfine coupling constants/ $10^{-4}$  cm<sup>-1</sup>. Absolute values only are given. <sup>b</sup> Reference 19b. <sup>c</sup> Reference 19a.

The specific assignment of pyrrole resonances, demonstrated for Ni<sup>II</sup>(STPP)Cl,<sup>26</sup> could not be achieved by <sup>2</sup>H NMR investigations. The upfield shift of the thiophene resonance, observed for copper(II) and nickel thiaporphyrins (Table 1), is related to the characteristic side-on coordination of the thiophene moiety. Such coordination allows direct transfer of  $\sigma$ -spin density from the sulfur  $\sigma$ -pair into the thiaporphyrin  $\pi$  orbital system. The spread of pyrrole resonances and the upfield thiophene shift result from delocalization of the positive  $\pi$  density as the involved  $\pi$  orbitals extend over the entire ligand molecule. Assuming simple additivity of contact mechanisms, the upfield contribution reflects the  $\pi$ -orbital composition. Such a mechanism has been discussed in detail previously for Ni<sup>II</sup>(STPP)Cl<sup>26</sup> and Ni<sup>II</sup>(NCH<sub>3</sub>TPP)-Cl.<sup>31</sup> In the latter case an upfield shift of an N-methylated pyrrole has been observed. Previously we have established the influence of the nature of axial ligand(s) and the macrocyclic geometry on the pyrrole proton shifts for a series of Ni<sup>II</sup>(STPP)L<sub>*n*</sub> (*n* = 1 or 2) complexes.<sup>26,32</sup> The most sensitive resonance, assigned to the pyrrole ring *trans* to the thiophene moiety, presented a paramagnetic shift which varied in the range from +63 to -7 ppm (293 K). These changes reflected the number and nature of axial ligands. Ni(STPP)( $\sigma$ -phenyl) presented the very first case with an upfield pyrrole position for nickel thiaporphyrins.<sup>32</sup> The paramagnetic shifts of the *cis* pyrrole rings were perturbed to a smaller extent (Table 1). The  $\pi$  spin density at the *meso* position and on the phenyl rings of Cu<sup>II</sup>(STP)Cl may result from the delocalization within occupied orbitals or from extensive  $\pi$ -back-bonding of the fully occupied *d*<sub>*xz*</sub> and *d*<sub>*yz*</sub> orbitals into LUMO of the thiaporphyrin as discussed for Ni<sup>II</sup>(STPP)Cl.<sup>26</sup> The values of the contact shifts in both cases are very similar. The contact shift of the phenyl resonances increase when chloride is replaced by perchlorate.

The NMR spectra of Cu<sup>II</sup>(STPP)Cl clearly display characteristics that reveal typical shift patterns of five-coordinate d<sup>9</sup> metallothiaporphyrins. We have chosen to discuss the NMR spectrum of Cu<sup>II</sup>(STPP)Cl in detail in this paper, which is mainly concerned with nickel species, to establish a spectroscopic standard for the spin, electronic, and ligation states of nickel thiaporphyrins or nickel porphyrins by an NMR investigation where the structures are still the matter of consideration. All NMR features of Cu<sup>II</sup>(STPP)Cl are reproduced by five-coordinate Ni(STPP)L species. The logical conclusion that follows is that there are Ni(I) compounds at least in the case when NMR spectra are accepted as a criterion of the oxidation state in the nickel thiaporphyrins.

The NMR spectra of four-coordinate Ni(STPP-*d*<sub>6</sub>), Ni(STPP-*d*<sub>10</sub>), and Ni(SDPDTP-*d*<sub>2</sub>) are clearly different from those of the five-coordinate analogs. In particular we observed a considerable upfield shift (ca. 120 ppm, 298 K) accompanied by a sign flip for only one pyrrole resonance. Selectively, one set of phenyl resonances demonstrates the noticeable increase of  $\pi$ -spin density

that can be converted into a 5-fold increase in spin density at the 10,15 *meso* positions as the other two remain practically intact. On the basis of our previous conclusions, it is reasonable to expect that downfield shifts of two out of three pyrrole resonances are associated with delocalization through a  $\sigma$ -type molecular orbital. This implies population of (*ad*<sub>*xz*</sub> + *bd*<sub>*yz*</sub>) by an unpaired electron and a downfield shift due to a  $\sigma$ -mechanism. In the second extreme case the low-spin nickel(II) porphyrin  $\pi$ -anion radical structure has to be considered. The one electron occupation of the LUMO thiaporphyrin orbital ( $\psi_1$ , Figure 9, in ref 26) would produce large spin densities at thiophene, at the pyrrole *trans* to thiophene, and at *meso* positions. No  $\pi$ -spin density is located at the two remaining pyrrole positions. Such spin densities are expected to induce very characteristic NMR patterns: i.e., one upfield shifted pyrrole resonance, two pyrrole resonances at diamagnetic positions, and alternating upfield-downfield shifts for *meso* phenyls (*meta* downfield; *ortho*, *para* upfield). A similar NMR pattern was presented by the  $\pi$ -anion radical [Zn(TPP\*)]<sup>-</sup>.<sup>24</sup> In the case of Ni(STPP) the contact shifts can be interpreted as a hybrid which corresponds to two canonical forms, i.e., the typical five-coordinate NMR spectrum exemplified by Cu<sup>II</sup>(STPP)Cl (see above) and the hypothetical NMR spectrum of the low-spin Ni<sup>II</sup>(STPP)  $\pi$ -anion radical.

An alternative explanation is consistent with thiaporphyrin to nickel(I) charge transfer since the strong overlap between (*ad*<sub>*xz*</sub> + *bd*<sub>*yz*</sub>) metal orbitals and  $\pi$ -orbitals of the thiaporphyrin is expected. This would place spin density in the filled  $\pi$ -orbital (e.g.,  $\psi_9$  in Figure 9 of ref 26) with large spin density at the  $\beta_3$  pyrrole positions. Since the Ni-S bond is extremely short, this path should be quite effective. Simultaneously, acting metal to ligand charge transfer would place spin density on the LUMO of thiaporphyrin producing expected spin density at the *meso* positions. The difference of shifts between five-coordinate and four-coordinate species is related to the out-of-plane position of the metal ion with respect to the porphyrin plane: Ni(STPP), 0.042 Å; Ni<sup>II</sup>(STPP)Cl, 0.295 Å; Cu<sup>II</sup>(STPP)Cl, 0.247 Å.<sup>12</sup> One can expect that the nickel(I) ion is pulled out from the thiaporphyrin plane for the five-coordinate species, as observed in the analogous Cu<sup>II</sup>(STPP)Cl complex.

This geometrical change should stabilize the metal d orbitals with respect to the  $\pi^*$  ligand orbitals, which should increase the metal character of the SOMO.<sup>5,6e</sup> The observed upfield pyrrole and widely spread phenyl resonances seem quite unusual. One could be tempted to relate them solely with the anion radical nature of the system. However, relatively large values of contact shifts have been found for selected metalloporphyrins. The contact shifts of *meso* phenyls as established for Fe<sup>III</sup>(TPP)Cl<sup>33</sup> (*ortho*, -6.54, -5.65 ppm; *meta*, 3.15-3.56 ppm; *para*, -3.37 ppm) are comparable with contact shifts of Ni(STPP) (Table 1), but result from metal to ligand charge transfer into the LUMO of the

(31) Latos-Grażyński, L. *Inorg. Chem.* **1985**, *23*, 1681.

(32) Chmielewski, P.; Latos-Grażyński, L. *Inorg. Chem.* **1992**, *31*, 5231.

(33) Behere, V.; Birdy, R.; Mitra, S. *Inorg. Chem.* **1982**, *21*, 386.

porphyrin.<sup>22</sup> It produces large upfield contact shifts for *meso* protons in Fe<sup>III</sup>(OEP)Cl (-80.4 ppm)<sup>34</sup> and the corresponding alternating sign shift pattern for phenyls of Fe<sup>III</sup>(TPP)Cl. Noticeably large upfield pyrrole contact shifts are produced via ligand to metal charge transfer for Ru<sup>IV</sup>(TPP)Br<sub>2</sub> (56 pm).<sup>35</sup> The typical cases of metalloporphyrin  $\pi$ -radical structure, i.e. iron porphyrin  $\pi$ -cation radicals<sup>36</sup> or ruthenium(II)  $\pi$ -cation radicals,<sup>35</sup> are characterized by larger limiting phenylshift values than those established for Ni(STPP).

## Conclusion

A combination of EPR and <sup>2</sup>H NMR studies have provided an electronic and structural characterization of copper(II) thiaporphyrins and nickel(I) in a thiaporphyrin ligand environment. A parallel analysis of <sup>61</sup>Ni hyperfine coupling constants and isotropic shift values offers direct and valuable insight into the spin density distribution in reduced nickel macrocycles.

The results presented here have implications involving the electronic structure of the Ni(I) complexes in general. In terms of two canonical structures, i.e. nickel(I) macrocycle or nickel(II)  $\pi$ -anion macrocyclic radical, the experimentally observed electronic unpaired electron distributions seem to reflect both features simultaneously as the orbital containing unpaired electron (SOMO) involves comparable contributions of ligand and metal character.

In light of our investigation, we would like to point out that large anisotropy of the *g* tensor in reduced nickel macrocycles does not necessarily give definitive proof of the *dominating* spin density localization on the nickel center. The tendency to discuss the electronic structure in terms of two simple canonical forms seems to be rather simplified. In a sense, one can describe these and similar compounds at metallomacrocyclic radicals which are analogs of metallorganic anion radicals<sup>36-38</sup> with varied metallic contribution to the SOMO.

## Experimental Section

**Solvents and Reagents.** <sup>61</sup>Ni was obtained as the metallic powder (90.4% enriched) from Technabexport and converted into anhydrous <sup>61</sup>NiCl<sub>2</sub>. All common solvents were thoroughly dried and distilled under nitrogen prior to use. Sodium anthracene was synthesized as previously described.<sup>39</sup> Benzene-*d*<sub>6</sub> (IBJ) and toluene-*d*<sub>8</sub> (Isotopes) were dried over molecular sieves. Axial ligands—pyridine, 1,2-dimethylimidazole (Merck), 1-methylimidazole (Aldrich), methylidiphenylphosphine (Aldrich), ethyldiphenylphosphine (Aldrich), and triethyl phosphite (Fluka)—were used as received. Sulfur dioxide was generated from sodium sulfite with sulfuric acid by a standard procedure. Silver perchlorate (Aldrich) was recrystallized from acetonitrile and dried in very small portions directly before use.

**Preparation of Compounds.** ST(R)PPH. Tetraphenyl-21-thiaporphyrin and its derivatives were synthesized as described recently.<sup>11a</sup>

STPPH-*d*<sub>10</sub>. Selectively deuterated 5,20-diphenyl-10,15-bis(phenyl-*d*<sub>5</sub>)-21-thiaporphyrin was synthesized using benzaldehyde-*d*<sub>5</sub>, which was obtained by oxidation of toluene-*d*<sub>8</sub> with Ce(SO<sub>4</sub>)<sub>2</sub>.<sup>40</sup>

STPPH-*d*<sub>6</sub> (deuterated at pyrrole  $\beta$ -positions) was prepared from pyrrole-*d*<sub>5</sub>.<sup>29,41</sup> Partial deuteration of the thiophene  $\beta$ -position was established in the course of this procedure.

SDSPDTPH-*d*<sub>2</sub> (85% deuterated at the  $\beta$ -thiophene position) was synthesized in the same manner as SDPDTPH by the condensation of 2,5-bis((phenylhydroxy)methyl)thiophene-*d*<sub>2</sub>, pyrrole, and *p*-tolylaldehyde.<sup>11a</sup> Coupling of 1-phenyl-2-propyn-1-ol according to the standard procedure gave 1,6-diphenylhexa-2,4-diyne-1,6-diol.<sup>42</sup> The required precursor deuterated at the thiophene  $\beta$ -position, 2,5-bis((phenylhydroxy)methyl)thiophene-*d*<sub>2</sub> was obtained according to the procedure described for 2,5-bis((phenylhydroxy)methyl)thiophene<sup>43</sup> from 1,6-diphenylhexa-2,4-diyne-1,6-diol and deuterium sulfide (D<sub>2</sub>S). The reaction of the thiophene ring formation was carried out in absolute ethanol-*d* (C<sub>2</sub>H<sub>5</sub>OD) saturated with D<sub>2</sub>S. The modification resulted in the placement of deuterium in the  $\beta$ -position (90% based upon the <sup>1</sup>H NMR spectrum).

**Synthesis of Nickel and Copper Thiaporphyrins.** Ni<sup>II</sup>(STPP)Cl and Cu<sup>II</sup>(STPP)Cl complexes and all deuterated derivatives were prepared as described recently.<sup>26,29,44</sup> Cu<sup>II</sup>(STPP)(ClO<sub>4</sub>) was generated directly in NMR tube by titration of Cu<sup>II</sup>(STPP)Cl with Ag(ClO<sub>4</sub>). <sup>61</sup>Ni(II) complexes were synthesized in a similar procedure, but a 5-fold excess of thiaporphyrin with respect to <sup>61</sup>NiCl<sub>2</sub> was used. Ni<sup>II</sup>(STPP)Cl was reduced to Ni(STPP) with zinc amalgam in benzene and recrystallized from acetonitrile.<sup>11</sup> Direct reduction in the NMR tube was carried out with sodium anthracene or tetrabutylammonium borohydride (Aldrich).

**Sample Preparation.** The concentrations of the samples used were 0.2 mg/cm<sup>3</sup> for EPR and 10 mg/cm<sup>3</sup> for <sup>2</sup>H NMR. Samples were deoxygenated directly in EPR or NMR tubes by bubbling N<sub>2</sub> through teflon tubing immersed in the sample and sealed with a septum cap. Solutions used for titration were deoxygenated as described by syringe technique. Gastight syringes were used for titration. A positive pressure of N<sub>2</sub> was kept during addition of reagents.

**Instrumentation.** <sup>1</sup>H NMR and <sup>2</sup>H NMR spectra were measured on a Bruker AMX 300 spectrometer operating in a quadrature detection mode (<sup>1</sup>H, 300 MHz; <sup>2</sup>H, 46.06 MHz). Usually 10 000 scans were accumulated with a delay time of 50 ms for each <sup>2</sup>H NMR spectrum. The spectra were collected over a 30-kHz band width with 4K data points. The signal to noise ratio was improved by apodization of the free induction decay which induced typically 25–50 Hz broadening. Both 5- and 10-mm probes were used. The peaks were referenced against residual solvent resonances.

EPR spectra were obtained with a Radiopan 8E/X spectrometer. The magnetic field was calibrated with a proton magnetometer and EPR standards. The following conditions were routinely used to record NMR spectra: microwave power 2–20 mW, modulation amplitude 1–5 G, frequency 9.17 GHz. The EPR spectra were simulated assuming orthorhombic symmetry. In the spectra of samples enriched in <sup>61</sup>Ni the 10% contribution of the <sup>58</sup>Ni isotope was taken into account in the simulation procedure.

The respective program summed spectra due to all possible orientations weighted by the solid angle element  $-\frac{1}{2}\Delta(\cos\theta)\Delta\phi$  and the orientation dependent transition probability which was calculated according to Aäsa and Vängård<sup>45</sup> for each particular transition. The best fit has been obtained with a Gaussian line shape. The fitting procedure was based on Marquardt's method,<sup>46</sup> i.e. using a minimization procedure with respect to square deviations of the theoretical and experimental signal intensities calculated for 500 field values.

**Acknowledgment.** Financial support of the State Committee for Scientific Research KBN (Grant 2 0732 91 01) is gratefully acknowledged.

(34) La Mar, G. N.; Eaton, G. R.; Holm, R. H.; Walker, F. A. *J. Am. Chem. Soc.* **1973**, *95*, 63.

(35) Rachlewicz, K.; Latos-Grażyński, L. *Inorg. Chim. Acta* **1988**, *144*, 213.

(36) (a) Gans, P.; Marchon, J.-C.; Reed, C. A.; Regnard, J.-R. *Nouv. J. Chim.* **1981**, *5*, 203. (b) Phillippi, M. A.; Goff, H. M. *J. Am. Chem. Soc.* **1982**, *104*, 6026. (c) Goff, H. M.; Phillippi, M. A. *J. Am. Chem. Soc.* **1983**, *106*, 756.

(37) (a) DeGray, J. A.; Geiger, W. E.; Lane, G. A.; Rieger, P. H. *Inorg. Chem.* **1991**, *30*, 4100. (b) Connelly, N. G.; Geiger, W. E.; Lane, G. A.; Raven, S. J.; Rieger, P. H. *J. Am. Chem. Soc.* **1986**, *108*, 6219.

(38) Goldberg, K. I.; Bergman, R. G. *J. Am. Chem. Soc.* **1988**, *110*, 4853.

(39) (a) Paul, D. E.; Lipkin, D.; Weissman, S. I. *J. Am. Chem. Soc.* **1956**, *78*, 116. (b) Hirota, N. *J. Am. Chem. Soc.* **1968**, *90*, 3603.

(40) Syper, L. *Tetrahedron Lett.* **1966**, 4493.

(41) Boersma, A. D.; Goff, H. M. *Inorg. Chem.* **1982**, *21*, 581.

(42) Eglinton, G.; McCrae, W. *Adv. Org. Chem.* **1963**, *4*, 225.

(43) Ulman, A.; Manassen, J. *J. Am. Chem. Soc.* **1975**, *97*, 6540.

(44) Latos-Grażyński, L.; Lisowski, J.; Olmstead, M. M.; Balch, A. L. *Inorg. Chem.* **1989**, *28*, 1183.

(45) Aäsa, R.; Vängård, T. *J. Magn. Reson.* **1975**, *19*, 308.

(46) Marquardt, D. W. *SIAM J.* **1963**, *11*, 431.